

Accurate Virus Quantitation Using a Scanning Transmission Electron Microscopy (STEM) Detector in a Scanning Electron Microscope

Candace D Blancett¹, David P Fetterer², Keith A Koistinen^{1,6}, Elaine M Morazzani^{3,5}, Mitchell K Monninger¹, Ashley E Piper³, Kathleen A Kuehl¹, Brian J Kearney⁴, Sarah L Norris², Cynthia A Rossi⁴, Pamela J Glass³, Mei G Sun^{1,*}

¹Pathology Division, United States Army Medical Research Institute of Infectious Diseases (USAMRIID), 1425 Porter Street, Fort Detrick, Maryland, 21702

²Biostatistics Division, United States Army Medical Research Institute of Infectious Diseases (USAMRIID), 1425 Porter Street, Fort Detrick, Maryland, 21702

³Virology Division, United States Army Medical Research Institute of Infectious Diseases (USAMRIID), 1425 Porter Street, Fort Detrick, Maryland, 21702

⁴Diagnostics Systems Division, United States Army Medical Research Institute of Infectious Diseases (USAMRIID), 1425 Porter Street, Fort Detrick, Maryland, 21702

⁵Current Address: General Dynamics Information Technology, 321 Ballenger Center Drive, Frederick, Maryland, 21702

⁶Current Address: Army Public Health Center, Toxicology Directorate, 5158 Blackhawk Road Aberdeen Proving Ground, MD 21010-5403

*Corresponding Author

Abstract

A method for accurate quantitation of virus particles has long been sought, but a perfect method still eludes the scientific community. Electron Microscopy (EM) quantitation is a valuable technique because it provides direct morphology information and counts of all viral particles, whether or not they are infectious. In the past, EM negative stain quantitation methods have been cited as inaccurate, non-reproducible, and with detection limits that were too high to be useful. To improve accuracy and reproducibility, we have developed a method termed Scanning Transmission Electron Microscopy – Virus Quantitation (STEM-VQ), which simplifies sample preparation and uses a high throughput STEM detector in a Scanning Electron Microscope (SEM) coupled with commercially available software. In this paper, we demonstrate STEM-VQ with an alphavirus stock preparation to present the method's accuracy and reproducibility, including a comparison of STEM-VQ to viral plaque assay and the ViroCyt Virus Counter.

Keywords: Scanning Transmission Electron Microscopy Detector, Virus Quantitation

1. Introduction

Quantitation is an important factor when studying the environmental impact of viruses, or virus impact on a specific host¹⁻³. An accurate method for the quantitation of virus particles would be very useful, but a universally accepted method has not been adopted by the scientific community¹⁻⁴. Routinely, multiple different methods of quantitation have been used to substantiate the validity of the other methods. Commonly used methods for virus quantitation includes negative staining Transmission Electron Microscopy (TEM) counting, agar overlay plaque assay, quantitative reverse transcription-polymerase chain reaction (qRT-PCR), immunofluorescence microscopy, Endpoint dilution assay (TCID₅₀) and analytical flow cytometry^{1-3,5,6}. Direct EM quantitation is a valuable technique because it provides enumeration of all virus particles, those

that are infectious, and those that are non-infectious^{2,3,7}. However, standardized methods for EM virus quantitation have not been universally implemented, and current techniques can yield inconsistent results with a low limit of detection^{2,3,6}. To address the shortcomings of inconsistency and limit of detection, we developed the STEM-VQ method. This is an efficient, reproducible SEM quantitation method which combines mPrep/g capsules to improve and simplify sample preparation with a STEM detector in an SEM for automated image acquisition⁸. TEM particle counting was first documented in the 1940s using a spray or centrifugation technique to deposit the sample on the supporting media, followed by negative staining with 2% Uranyl Acetate^{2,9-12}. Virus particles within representative fields were imaged with a TEM and manually counted. The final concentration was calculated based on the area imaged and the volume of sample applied^{9,10,12-16}. Since that time, scientists have continued to adapt application techniques to improve sample distribution and different purification steps to decrease sedimentation that interfered with imaging and counting^{14,15}. In 1950, scientists began using a known concentration of latex beads as a reference within their sample. This allowed calculations based on the bead concentration instead of the area imaged¹⁰⁻¹³. Inclusion of these reference beads led to development of the droplet method for sample application¹². Several variations have been developed, but the most common method involves placing a drop of sample onto a horizontally oriented grid^{12,16}. While other methods of counting have been used, typically, the two main approaches for counting TEM images involve either counting a set number of grid squares or a set number of beads. Thresholds for each of these methods have been as few as 3 grid squares, or 200 beads, respectively^{2,16}. There have been numerous approaches to calculating the final concentration of virus^{2,3,5,6,13-16}. With the development of image analysis software and more automated microscopes in recent years, automated image acquisition, analysis, and

enumeration has emerged ¹. SEM has been used for many years in the quantitation of particles for material sciences samples and STEM imaging has been used for particle counting in cell monolayers, but STEM imaging has not gained widespread use for particle counting material in biology or virology fields ^{1,17-20}.

We have developed a consistent, reproducible virus quantitation method called STEM-VQ which simplifies sample preparation and utilizes large throughput STEM detector in the SEM for imaging, and commercially available image analysis software. Briefly, our method continues to use a known concentration of gold beads as a reference, but it involves an different application method with three major steps (Figure 1A): First, an equal volume of gold beads is mixed with an unknown concentration of virus particles and the mixture is applied to the EM grid using mPrep/g capsules^{8,12,21,22} (Supplementary Figure 1). Use of the mPrep/g capsules reduces direct handling of grids and allows easy application of samples and buffers. Second, the grids are imaged with a STEM detector in the SEM using the automated ATLAS software. Compared to traditional TEM imaging, STEM detector imaging in the SEM eliminates the need for negative staining and allows easy imaging of a much larger portion of the grid. Third, ImageJ image analysis software is used to enumerate virus and gold particles. These counts are used to determine the virus to gold ratio and calculate the original virus concentration (Figure 1C). In this study, we present a comparison of the STEM-VQ method to agarose-based viral plaque assay and the ViroCyt Virus Counter 2100 (VC) (ViroCyt, Boulder, CO, USA) ^{3,23}.

2. Material and Methods

2.1. Virus suspension preparation

Venezuelan Equine Encephalitis virus (VEEV), INH-9813 strain and Eastern Equine Encephalitis virus (EEEV), V105-00210 strain were received from Dr. Robert Tesh at the University of Texas Medical Branch repository. VEEV INH-9813 was isolated from the serum of an infected individual who presented with clinical symptoms in Columbia, South America in 1995²⁴. The virus was isolated following a single passage in Vero cells. EEEV V105-00210 was isolated from a human case in Massachusetts in 2005, with no passage in animals and a single passage in cell culture²⁵. Western Equine Encephalitis virus (WEEV) McMillan strain was received from the Centers for Disease Control and Prevention, Fort Collins, CO. This virus was originally isolated from a human case in Ontario, Canada in 1941²⁶. This virus had a passage history in both animals and cell culture. Biosafety Level (BSL-3) laboratory prepared master virus stocks (MVS), working virus stocks (WVS), and sucrose purified virus stocks (SpVS) virus stocks were prepared using ATCC Vero 76 cells. For MVS and WVS, Vero cells were infected at a multiplicity of infection (MOI) of 1 in Eagles Minimal Essential Medium (EMEM, Cellgro) containing 2% fetal bovine serum (FBS, HyClone), 1% non-essential amino acids (NEAA, Gibco), 1% Penicillin-Streptomycin (Pen-Strep, 10,000 U/ml and 10 mg/ml stock, respectively, Sigma-Aldrich), 1% HEPES buffer (1M stock, Sigma-Aldrich), and 1% L-glutamine (200 mM stock, HyClone). At 24-32 hours post-infection (PI), culture supernatants were harvested and clarified by centrifugation at 10,000 x g for 30 minutes (Sorvall GSA rotor). Virus stocks were aliquoted and stored at -70°C for future use. The SpVS, supernatant was collected from Vero cells that were infected at a MOI=1 in EMEM containing 5% FBS, 0.5% Pen-Strep (stock solution above), 1% HEPES (stock solution above), 1% L-Glutamine (stock solution above), and 0.1% Gentamicin (50 mg/ml stock, Sigma-Aldrich) and clarified by centrifugation. Virus was precipitated with 2.3% NaCl and 7% Polyethylene glycol (MW8000,

Sigma-Aldrich), with stirring, overnight at 4°C. Virus was pelleted by centrifugation at 10,000 x g for 30 minutes (Sorvall GSA rotor). Virus pellets were resuspended in 1x TNE Buffer (10 mM Tris, 0.2 M NaCl, 1 mM EDTA, pH 7.4) and layered onto 20-60% continuous sucrose density gradients. This was spun at 100,000 x g, 4°C, for 4 hours (SW-28Ti rotor, Beckman). The virus band was collected, aliquoted and stored at -70°C for future use.

For all stocks, deep sequence analysis determined that the sequence of these isolates were consistent with the reported strain of VEEV, EEEV, and WEEV. Additionally, this sequencing analysis demonstrated that the virus stocks did not contain contaminating agents.

2.2.STEM-VQ sample preparation with mPrep/g capsules

Viral stocks were serially diluted at 1:10 in phosphate buffered saline (PBS) with dilution volumes of at least 5 ml to achieve the final dilution for application to EM grids. Two formvar-carbon coated 200 mesh copper EM grids (SPI, Cat#3420C-MB) were inserted into a capsule based-microscopy processing system called mPrep/g⁸ (Figure 1A left, Microscopy Innovation, LLC, WI, Cat#G1600 and F1602). Gold beads (40nm, Ted Pella Cat#15707-5, 1.461E10 particles/ml concentration certified by Particle Technology Labs) were sonicated for 10 minutes and transported into biocontainment with grid-loaded mPrep/g capsules along with filters, fixatives, and 1% osmium tetroxide. Step 1, in the biocontainment suite, equal volumes of virus (unknown concentration) and gold beads (known concentration) were well mixed (Figure 1B) and 40µl of the resulting suspension aspirated into the mPrep/g capsule while attached to a pipette (Figure 1A left). Step 2, the pipette with mPrep/g attached was laid on its side for 10 minutes with grids oriented horizontally for even sample distribution onto grid formvar. Step 3, the pipette was picked up and the plunger pressed to dispense the virus bead mixture into a waste

container. An aliquot (40 μ l) of fixative (2% glutaraldehyde in water) was then aspirated into capsule, incubated with grids oriented horizontally for 20 minutes, and then dispensed into a waste container. Three rinse cycles were performed by aspirating and immediately dispensing 40 μ l of deionized (dI) water. An extra ten rinse cycles were needed with samples that were dense such as the SpVS conditions. Step 4, the mPrep/g capsule was removed from the pipette and placed, with the lid open, into a 50ml centrifuge tube containing filter paper soaked in 1% Osmium Tetroxide (OsO₄) suspended in water. The tube was sealed for 1 hour to ensure complete inactivation of the virus by OsO₄ vapor and transferred to the BSL-2 electron microscopy facility. Step 5, in the BSL-2 EM facility the mPrep/g capsule was removed from the tube and placed onto a pipette. Three rinse cycles were repeated by aspirating 40 μ l of dI water followed by dispensing into a waste container. The capsule was removed from the pipette, lid opened, and allowed to air dry. Once dry, the grids were ready to be imaged under STEM detector in the SEM. (Supplementary Figure 1) Note, Step 4, inactivation with osmium tetroxide vapor, can be eliminated for samples that do not require BSL-3 or -4 biocontainment.

2.3.STEM imaging

TEM grids were loaded into a Zeiss Sigma Field Emission SEM and imaged with a STEM detector at 30kV. Images were auto-acquired using Zeiss FIBICS ATLAS software: using 35X35 μ m frame size, 4nm/pixel spacing, and 2000ns dwell time.

2.4.Data analysis by ImageJ

ImageJ software was used to individually count alphaviruses (~70nm in diameter) and nano-gold particles (~40nm in diameter) according to their respective particle sizes. Suggested ImageJ macro codes are recorded in supplementary figure 3.

2.5.STEM-VQ Statistical Analysis

Virus to bead ratio:

For each grid, the virus to bead' ratio was estimated as the slope of the linear regression of the virus to bead count per sampled grid area, forced through the origin. The sampling variance of the estimated virus to bead ratio obtained from a single grid was taken from the large sample delta-method approximation, as discussed by Kempen and Vilet ²⁷.

$$var(r_1) \approx \frac{1}{n} \left(\frac{var(x)}{\mu_y^4} + \frac{\mu_x^2 var(y)}{\mu_y^4} - \frac{2\mu_x cov(x,y)}{\mu_y^3} \right)$$

Where x and y are the bead count and the bead weighted virus count and n is the number of sampled areas. Multiple grids were examined per virus sample, an average of the log virus to bead ratio is formed by linear mixed model. This procedure reweights the average to adjust for the correlation observed between certain sets of grids, as well as sampling variances within grid. Analysis was performed using the PROC MIXED procedure in SAS Version 9.4.

Calculation of the concentration of particles:

The following formula is used to calculate the concentration of particles:

$$\text{Unknown Virus Concentration} = \text{Virus to bead ratio} \times \text{Known bead Concentration}$$

2.6.Agarose Overlay Plaque Assay

Each virus stock was quantitated by standard agarose overlay plaque assay²³. Virus stocks were serially diluted in Hank's Balanced Saline Solution (HBSS). ATCC Vero 76 cells seeded on 6-well plates were grown to 90-100% confluence. Duplicate wells were infected with 100µL/well

of each serial dilution. Plates were incubated at 37°C for 1 hour, with rocking every 15 minutes for even distribution and to keep the monolayer from drying. Following the incubation period, wells were overlaid with 0.5% agarose in 2X Eagle's Basal Medium with Earle's Salts (EBME, USAMRIID, Fort Detrick, MD) containing 1% HEPES and 10% FBS, 1% L-glutamine, 1% NEAA, 1% Pen-Strep, and 0.1% gentamycin, and plates incubated at 37°C with 5% CO₂. After twenty four hours the cells were stained with the addition of a second agarose overlay prepared as above with 5% neutral red (Gibco). The plates were incubated at 37°C with 5% CO₂ for an additional 24 hours. Infectivity was quantitated by counting defined plaques (neutral red exclusion areas). Titer was calculated by factoring in the volume of inoculum used per well and the dilution(s) with plaque counts between 10 and 150.

2.7. ViroCyt Quantitation

Samples were tested on the VC using the ViroCyt reagent kit and following manufacturer's instructions. The strategy was similar to that described for filoviruses in Rossi *et al.*, 2015³. Virus preparations were diluted beginning at 1:10 into ViroCyt sample buffer. Serial ¼ log dilutions were prepared from the 1:10 in order to provide samples with values within the linear range of the VC. Briefly, 300µl of each dilution was stained using 150µl of Combo Dye solution, incubated in the dark at room temperature for 30 minutes, and analyzed in the VC. Each dilution was tested in triplicate with inter-sample washes and a cleanliness control run between each sample to verify the flow path was clean. Results were automatically analyzed by the instrument software and reported as virus particles per ml (VP/ml). The sample quantitation limit (SQL) for unpurified virus stocks were similar to that previously reported for filoviruses (2.0E+06 VP/ml) while purified virus SQL was lower and equivalent to the lower limit of the linear range of the instrument (5.5E+05 VP/ml). All VC results greater than this value were

considered statistically distinguishable from background and therefore reportable. Final virus particle concentrations were established using all samples whose VP/ml counts were above background and within the linear range of the instrument. Microsoft Excel 2007 (Redmond, WA, USA) was used for linear-regression analysis and determining coefficient of variation between replicates. Instrument performance was validated prior to testing samples by running a manufacturer's control of known concentration.

3. Results

3.1. Sample preparation quality correlated with accuracy.

Uniform particle distribution and minimal background on EM grids was critical for achieving accurate results (Figure 2A, 2D)^{5,6,16}. Proper sample preparation, including bead agitation, extensive mixing of the gold beads with the virus, and at least 3 washes with reagent grade water was required. Particles aggregation was always a sample preparation problem (Figure 2B). Sonication of the bead stock prior to mixing with the virus helped to suspend the bead solution and eliminate clumping that formed when the solution was stored for a lengthy period between uses. Thorough mixing of the virus and gold beads by pipetting the mixture up and down several times evenly distributed sample throughout the solution and helped remove any viral aggregation. Nutrient rich media was required for virus growth, but this media resulted in crystallized salt and sugar deposits on the grid which made imaging and counting difficult (Figure 2C, 2E). Extra rinsing at least 10 times with water helped eliminate these deposits. Upon data analysis, we found that correlation strength between the gold bead count and virus count was an indicator of good sample preparation quality; and therefore, result accuracy (Figure 2D, 2E). All of the samples used here were well prepared and the standard macro was used. As

we have developed this method we have observed that while inferior preparations should be immediately identifiable during imaging, areas within the grid that contain particle clumping or dirty background may go undetected with our automated imaging process. Samples that contained particle aggregation or dirty background are usually identified by the technician when the data set is poorly correlated or contains extreme outliers (Figure 2E). In this event, the image analysis can be adjusted in a manner appropriate to the severity of the issue. Adjustments to the analysis macro code (Supplementary Figure 3) such as tailored thresholding or background extraction often solves the issue. If the particle aggregation or dirty background is severe enough a new grid preparation for imaging is required.

3.2.Computing bootstrapped standard error to statistically determine the number of images for an accurate STEM-VQ calculation.

One-hundred areas were imaged from a single grid to determine the number of imaged areas that would be required for an accurate representation of the entire grid (Figure 3A). Two possible estimators of the virus to bead ratio were compared: (1) the ratio of mean virus count to mean bead count (ratio of means) and (2) the slope of the linear regression of virus to bead counts, forced through the origin (regression through the origin). The 100 areas were resampled 50 times with replacement to form a boot-strap estimate of the standard error (Figure 3B)²⁸. As shown in Figure 3B, the standard error decreased with increasing numbers of sampled areas. Considering a compromise between the costs of increased sampling versus the reduction in error, we determined that 30 imaged areas per grid were needed for accurate quantitation. Most of the gains in reliability were realized by n=30, with further increases in the number of sampled areas yielding only small reductions in variance.

3.3. Individual sample preparations result in variation and limited analytical errors.

We found that a major source of error came from the variability between sample preparations. We analyzed 4 different preparations of 3 different individual VEEV stock samples. Each preparation consisted of two duplicate grids (Figure 4A). The results from the simultaneously prepared duplicate grids in each preparation were very similar to each other, but there were variations between different preparations. Figure 4B shows the standard error calculated from the counts in Figure 4A. The range varied between one standard error above and one standard error below demonstrating that the variability was less than a log, which is commonly considered acceptable for EM particle counts^{2,3,29}.

3.4. Detection limit for accurate counting

The detection limit for any EM procedure is typically considered $1\text{E}+07$ particles/ml (P/ml).^{2,6} In order to determine the range for accurate counting for the STEM-VQ method, we examined serial dilutions using alphavirus samples (Figure 5A). We found that samples containing greater than $1\text{E}+12$ P/ml typically had too much viral aggregation for an accurate quantitation (data not shown). At the lower end, samples below $1\text{E}+07$ P/ml had too few viral particles in the field of view for an accurate count (data not shown). Particle counts within the range of $1\text{E}+09$ to $1\text{E}+12$ P/ml provided accurate detection in 10-fold dilutions for three different sucrose-purified virus stocks (EEEV, WEEV and VEEV) (Figure 5B). All data in serial dilutions were linear, indicating the accuracy of the data set.

3.5. STEM-VQ method results were comparable to agarose-based plaque assay and ViroCyt Virus Counter results.

There are many ways to quantify virus, all of which use very different methods to identify particles. Among all methods, plaque assay and the VC are well developed and widely used. Plaque assay is the most common approach to virus quantitation and is typically considered the “gold standard”^{2,3}. It measures infectious virus particles by counting the number of plaques formed when virus is applied to a monolayer of cells, giving a count expressed as plaque forming units per ml (PFU/ml)²⁻⁴. The VC is a flow-based counter which quantifies virus particles in solution³. It requires the sample to be stained for protein and nucleic acid and counts particles containing both stains as intact virus particles, resulting in a count expressed as virus particles per ml VP/ml³. With STEM-VQ particle images are captured and particles counted electronically, then visually confirmed. Counts are expressed as particles per ml P/ml².

We compared STEM-VQ, plaque assay and VC results for different alphavirus stocks (Figure 6). The linear range of the VC was verified to be between 5.5E+05 and 1E+09 VP/ml. Testing of each virus prep resulted in a linear curve with $R^2 \geq 0.972$, slopes between 0.916 and 1.396 and coefficient of variation (%CV) $\leq 29\%$ using at least 4 concentrations and n between 11 and 18. Since the plaque assay measures infectious particles and the VC counts essentially intact virus particles, we expected VC and plaque assay results to be similar for each virus stocks. Our data agreed with this theory. We also expected the STEM-VQ results to be higher than both plaque assay and the VC since STEM-VQ counts the presence of all particles within a size range and cannot determine if they are infectious. We consistently found STEM-VQ results approximately 1.5 logs higher than the plaque assay and VC results (Figure 6). We do not propose that all types of viruses or variable conditions would result in a 1.5 log difference in plaque assay and EM counting, but we would always expect the EM count to be higher than plaque assay.

4. Discussion:

Virus quantitation using negative stain TEM imaging has been criticized as difficult and time consuming; issues we wanted to improve with the development of this method. In supplementary Figure 2, we compared and summarized the improvements made to the STEM-VQ method compared to the conventional TEM method. We simplified sample preparation with better distribution by using mPrep/g capsules in the process. The mPrep/g is a small capsule that functions as a pipette tip capable of holding two EM grids³⁰ (Figure 1A left). Once the grids have been inserted into the capsule, the person preparing the sample simply attaches the mPrep/g capsule to a pipette and no further grid manipulation is needed. Using mPrep/g resulted in much less damage to the grid during sample preparation, providing more data available to collect for more accurate results. It also made sample preparation in biocontainment labs (BSL3 and BSL4) much safer and easier. Each capsule holds 2 grids; therefore, duplicate grids can be made with no further effort. The capsules can also easily be loaded onto a multi-channel pipette, or stacked, so many samples or several replicates of the same sample can easily be prepared³⁰. Additionally, uniform particle distribution on the grid is critical for achieving accurate data^{5,6,16}. We found samples prepared using the capsule consistently showed more uniform distribution than samples prepared using the traditional droplet method⁸.

Our new automated imaging and analysis procedure saved valuable technician time and allowed for the collection of larger data set in a shorter period of time. ATLAS automated imaging software enabled the user to select multiple areas to image, optimize the image acquisition settings for quality imaging such as focus, brightness, and contrast, and then the software automatically acquired images from large areas of the sample while unattended. We were able to acquire images of thirty 35x35 μ m square areas from a 200 mesh grid in less than 3 hours, and a technician needed to be present for only 45 minutes of those 3 hours. This was significantly less

time when compared to traditional methods in which a technician must continually sit at the microscope manipulating the controls and taking individual images. This new method not only saved time but largely decreased the amount of hands-on time required by a technician.

Similarly, ImageJ analysis decreased the time needed to count the particles. Manually counting a well populated grid square requires hours of counting, whereas, using ImageJ software the same images were completed in less than 5 minutes. When counting or imaging is manually performed, accidental overlap or skipping an area frequently occurs. Utilization of software for analysis and automated image acquisition eliminated this error.

Virus quantitation is an important step when characterizing challenge material for use in animal models of infectious disease. There are many methods for virus quantitation including plaque assay, TCID₅₀, the VC, and EM^{1-3,5,6}. The desired information and practicality of each method should be considered when determining which method to use. The plaque assay can be time consuming, typically requiring many days to complete, and must be performed at the level of containment appropriate for the virus being handled^{2,3}. Choosing a cell line, media, and other variables are essential to a successful plaque assay³. Plaque assay has the lowest limit of detection³¹. It can only detect infectious particles, which a majority consider more applicable for dosing quantitation because infectious particles are responsible for disease; however, there is evidence that noninfectious particles can also effect the host immune response³². Therefore, it is important to evaluate noninfectious as well as infectious particles present in virus challenge stock preparations.

For alphaviruses, the VC results were comparable to plaque assay results, but VC has a higher limit of detection with an optimal range of 5.5E+5 – 1.0E+9 VP/ml³. It must also be operated in the level of containment required for the sample, but it was quick, taking less than an hour to

stain and count a sample. It was also the most affordable option, costing about \$5.00 per run.

However, the VC may provide poor results in samples with high levels of protein in the media ³.

A major limitation of EM counting methods despite improvements seen with the STEM-VQ method is the relatively high detection limit, a concentration of $1E+07$ P/ml remains necessary for accurate results ^{2,6}. Media containing high levels of salt, protein, or sucrose may lead to poor imaging if not properly rinsed, and poor fixation can lead to loss of sample from the grid or unidentifiable particles ^{2,5}. After BSL-3/-4 sample application to the grid, which takes about an hour, exposure to osmium tetroxide vapor quickly deactivates any virus and allows the rest of the work to be performed outside biocontainment ⁸.

Despite its challenges, EM quantitation is valuable due to its ability to count total virus particles and provide gross morphology data. It should be noted that although this method allowed for gross morphological evaluation; more detailed observations such as protein coat on virus particles requires additional EM procedures such as negative staining with TEM imaging. These EM methods can also be applied to other noninfectious nano-particles such as virus-like-particles (VLPs), whereas plaque assays and VC are unable to quantify VLPs. EM may also be able to provide insight into VLPs development or changes due to manipulations through morphologic evaluation ^{33,34}. STEM-VQ and VC particle counts can be used in conjunction with other quantitation methods, typically plaque assay, to create ratios that provide insight into both infectivity of a virus stock and the quality of the virus preparation. These ratios (P:PFU and VP:PFU) are important when examining alterations in the quality of virus stocks which can arise from mutation, poor handling techniques, or sequential passaging. ^{18,35,36}

The STEM-VQ method simplifies sample preparation, imaging, and data analysis for particle analysis using electron microscopy. These changes have increased the accuracy and reproducibility of the assay.

5. Acknowledgement:

We would like to acknowledge Dr. Camenzind Robinson (Janelia Research Campus, Howard Hughes Medical Research Institute) for his input and initial STEM set up for this project. We would like to thank SPC Joshua Patterson for helping proof read this manuscript. This work was funded in part by USAMRIID and the Defense Threat Reduction Agency-Joint Science and Technology Office (Program CB3691).

Opinions, interpretations, conclusions, and recommendations are those of the authors and are not necessarily endorsed by the U.S. Army.

Additional Information:

Competing financial interest statement: The authors declare no competing financial interests.

References:

1. Ferris, M.M., Stoffel, C.L., Maurer, T.T. & Rowlen, K.L. Quantitative intercomparison of transmission electron microscopy, flow cytometry, and epifluorescence microscopy for nanometric particle analysis. *Anal Biochem* **304**, 249-56 (2002).
2. Malenovska, H. Virus quantitation by transmission electron microscopy, TCID₅₀, and the role of timing virus harvesting: a case study of three animal viruses. *J Virol Methods* **191**, 136-40 (2013).
3. Rossi, C.A. *et al.* Evaluation of ViroCyt(R) Virus Counter for rapid filovirus quantitation. *Viruses* **7**, 857-72 (2015).
4. Bettarel, Y., Sime-Ngando, T., Amblard, C. & Laveran, H. A comparison of methods for counting viruses in aquatic systems. *Appl Environ Microbiol* **66**, 2283-9 (2000).
5. Kwon, Y.J., Hung, G., Anderson, W.F., Peng, C.A. & Yu, H. Determination of Infectious Retrovirus Concentration from Colony-Forming Assay with Quantitative Analysis. *J Virol* **77**, 5712-5720 (2003).

6. Reid, G.G. *et al.* Comparison of electron microscopic techniques for enumeration of endogenous retrovirus in mouse and Chinese hamster cell lines used for production of biologics. *J Virol Methods* **108**, 91-6 (2003).
7. Borsheim, K.Y., Bratbak, G. & Heldal, M. Enumeration and biomass estimation of planktonic bacteria and viruses by transmission electron microscopy. *Appl Environ Microbiol* **56**, 352-6 (1990).
8. Monninger, M.K. *et al.* Preparation of viral samples within biocontainment for ultrastructural analysis: Utilization of an innovative processing capsule for negative staining. *J Virol Methods* **238**, 70-76 (2016).
9. Sharp, D.G. Enumeration of virus particles by electron micrography. *Proc Soc Exp Biol Med* **70**, 54-9 (1949).
10. Backus, R.C. & Williams, R.C. The Use of Spraying Methods and of Volatile Suspending Media in the Preparation of Specimens for Electron Microscopy. *Journal of Applied Physics* **21**, 11-15 (1950).
11. Gelderblom, H.R., Renz, H. & Özel, M. Negative staining in diagnostic virology. *Micron and Microscopica Acta* **22**, 435-447 (1991).
12. Miller, M. Virus particle counting by electron microscopy. *Electron microscopy in biology* **2**, 305-339 (1982).
13. Kellenberger, E. & Arber, W. Electron microscopical studies of phage multiplication. I. A method for quantitative analysis of particle suspensions. *Virology* **3**, 245-55 (1957).
14. Mathews, J. & Buthala, D.A. Centrifugal sedimentation of virus particles for electron microscopic counting. *J Virol* **5**, 598-603 (1970).
15. Strohmaier, K. A new procedure for quantitative measurements of virus particles in crude preparations. *J Virol* **1**, 1074-81 (1967).
16. Zheng, Y.Z., Webb, R., Greenfield, P.F. & Reid, S. Improved method for counting virus and virus like particles. *J Virol Methods* **62**, 153-9 (1996).
17. Bogner, A., Jouneau, P.H., Thollet, G., Basset, D. & Gauthier, C. A history of scanning electron microscopy developments: towards "wet-STEM" imaging. *Micron* **38**, 390-401 (2007).
18. Carpenter, J.E., Henderson, E.P. & Grose, C. Enumeration of an extremely high particle-to-PFU ratio for Varicella-zoster virus. *J Virol* **83**, 6917-21 (2009).
19. Peckys, D.B. & de Jonge, N. Visualizing gold nanoparticle uptake in live cells with liquid scanning transmission electron microscopy. *Nano Lett* **11**, 1733-8 (2011).
20. Datye, A.K., Xu, Q., Kharas, K.C. & McCarty, J.M. Particle size distributions in heterogeneous catalysts: What do they tell us about the sintering mechanism? *Catalysis Today* **111**, 59-67 (2006).
21. Goodman, S.L. & Kostrna, M.S. Reducing Reagent Consumption and Improving Efficiency of Specimen Fixation and Embedding, Grid Staining and Archiving using mPrep Capsule Processing. *Microscopy and Microanalysis* **17**, 174-175 (2011).
22. Goodman, S.L., Wendt, K.D., Kostrna, M.S. & Radi, C. Capsule-Based Processing and Handling of Electron Microscopy Specimens and Grids. *Microscopy Today* **23**, 30-37 (2015).
23. Baer, A. & Kehn-Hall, K. Viral concentration determination through plaque assays: using traditional and novel overlay systems. *J Vis Exp*, e52065 (2014).
24. Weaver, S.C. *et al.* Re-emergence of epidemic Venezuelan equine encephalomyelitis in South America. VEE Study Group. *Lancet* **348**, 436-40 (1996).
25. Centers for Disease, C. & Prevention. Eastern equine encephalitis--New Hampshire and Massachusetts, August-September 2005. *MMWR Morb Mortal Wkly Rep* **55**, 697-700 (2006).
26. Nagata, L.P. *et al.* Infectivity variation and genetic diversity among strains of Western equine encephalitis virus. *J Gen Virol* **87**, 2353-61 (2006).

27. van Kempen, G.M. & van Vliet, L.J. Mean and variance of ratio estimators used in fluorescence ratio imaging. *Cytometry* **39**, 300-5 (2000).
28. Wasserman, L. in *All of Nonparametric Statistics* 27-39 (Springer-Verlag, New York, NY, 2006).
29. Darling, A.J., Boose, J.A. & Spaltro, J. Virus assay methods: accuracy and validation. *Biologicals* **26**, 105-10 (1998).
30. Goodman, S. & Kostrna, M. Reducing Reagent Consumption and Improving Efficiency of Specimen Fixation and Embedding, Grid Staining and Archiving using mPrep (TM) Capsule Processing. *Microscopy and Microanalysis* **17**, 1174 (2011).
31. Dulbecco, R. Production of Plaques in Monolayer Tissue Cultures by Single Particles of an Animal Virus. *Proc Natl Acad Sci U S A* **38**, 747-52 (1952).
32. Alfson, K.J. *et al.* Particle-to-PFU ratio of Ebola virus influences disease course and survival in cynomolgus macaques. *J Virol* **89**, 6773-81 (2015).
33. Pease, L.F., 3rd *et al.* Quantitative characterization of virus-like particles by asymmetrical flow field flow fractionation, electrospray differential mobility analysis, and transmission electron microscopy. *Biotechnol Bioeng* **102**, 845-55 (2009).
34. Roldao, A., Mellado, M.C., Castilho, L.R., Carrondo, M.J. & Alves, P.M. Virus-like particles in vaccine development. *Expert Rev Vaccines* **9**, 1149-76 (2010).
35. Thompson, K.A. & Yin, J. Population dynamics of an RNA virus and its defective interfering particles in passage cultures. *Virology* **7**, 257 (2010).
36. McCurdy, K. *et al.* Differential accumulation of genetic and phenotypic changes in Venezuelan equine encephalitis virus and Japanese encephalitis virus following passage in vitro and in vivo. *Virology* **415**, 20-9 (2011).

Figure Captions:

Figure 1: STEM-VQ Method overview. (A) The three major phases that are needed for determining particle concentration are illustrated: (left) sample preparation using mPrep/g system, (middle) STEM imaging in the SEM, (right) Particle counting using imageJ. (B) A mixture of a known concentration of gold beads with an unknown concentration of virus stock, followed by application of the mixture onto an EM grid for STEM imaging in the SEM is illustrated. (C) Formula used to calculate the number of unknown viral particles based on the known concentration of gold beads and the virus-gold ratio.

Figure 2: Good quality sample preparation produces data points that have a strong linear correlation: (A) An example of evenly distributed virus and beads. (B) This sample is to highly

concentrated, which leads to clumping and inability to determine an accurate count. (C) This sample contains large amount of crystal sediments and debris in the background; this background material is difficult to differentiate from viral particles when utilizing image analysis software. (D) A strongly correlated data set results from well prepared samples as in A, each data point, 10 total, represents the quantity of virus and beads in a $35 \times 35\mu\text{m}$ area on a single EM grid. (E) A poorly correlated data set indicates a poorly prepared sample as depicted in panels B and C, each data point, 10 total, represents the quantity of virus and beads in a $35 \times 35\mu\text{m}$ area on a single EM grid. Scale bars are 100nm.

Figure 3: Computing bootstrapped standard error to statistically determine the number of images required for an accurate STEM-VQ method. (A) Particle count data representing data from 100 imaged areas of a single grid. (B) Bootstrap estimates of the standard error computed by simulating 500 resamples of the 100 areas. Most of the reduction in error is achieved by 30 images.

Figure 4: Individual preparation causes small variations among the same virus stock sample. All counts are calculated from 30 different images per sample. (A) STEM-VQ particle count data of duplicate grids from 3 different individual virus stock samples prepared 4 different times. (B) Standard error from 4 different preparations for the 3 different individual virus stock samples.

Figure 5: STEM-VQ data from different sample dilutions indicate accurate counting result. All counts are calculated from 30 different images per sample. (A) Results from 3 different alphavirus stocks using 3 different dilutions. (B) Comparison of the data from different dilutions.

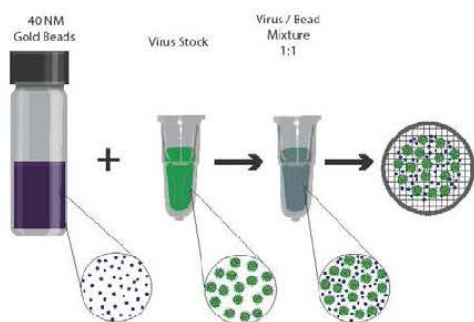
Figure 6: STEM-VQ method results are consistent with plaque assay and ViroCyt counting results. (A) Quantitation results for 5 different alphavirus stocks using 3 different quantitation methods. All EM counts are calculated from 30 different images per sample. (B) Comparison of the results from different methods in graphical format. EM results are higher than ViroCyt and plaque assay because it counts the presence of all particles, including non-infectious.

Figure 1

A



B



C

$$\left(\frac{\text{Virus Particle}}{\text{Bead}} \right)_{\text{Solution}} \approx \left(\frac{\text{Virus Particle}}{\text{Bead}} \right)_{\text{Grid}}$$

$$(\text{Virus Particle})_{\text{Solution}} \approx \left(\frac{\text{Virus Particle}}{\text{Bead}} \right)_{\text{Grid}} (\text{Bead})_{\text{Solution}}$$

Figure 2

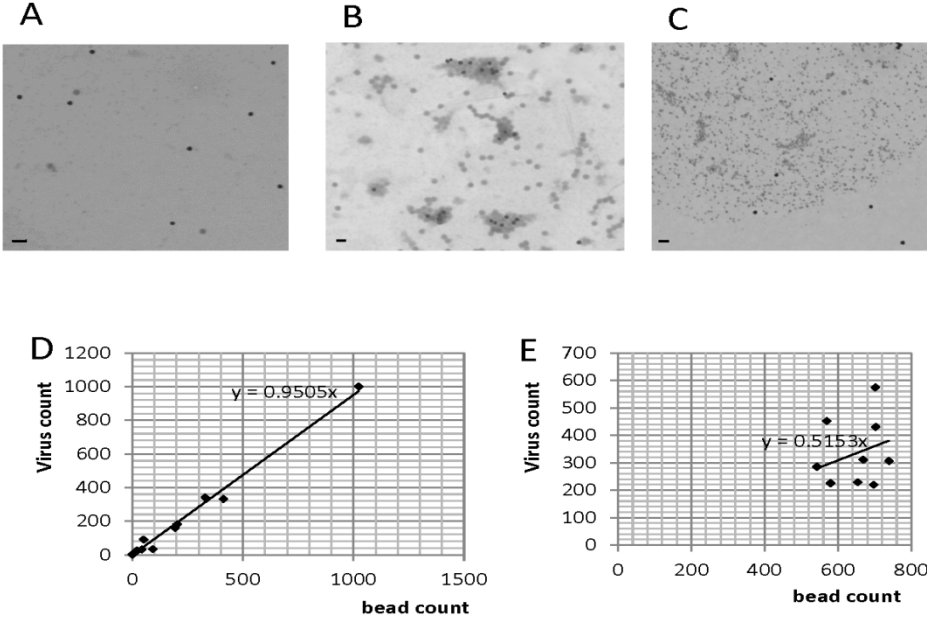


Figure 3

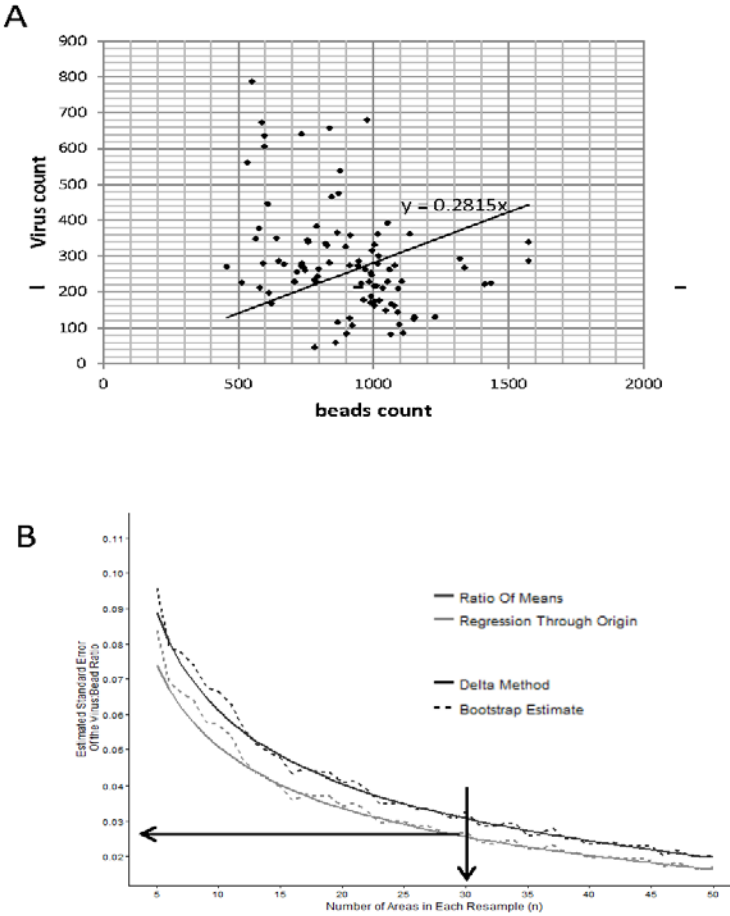


Figure 4

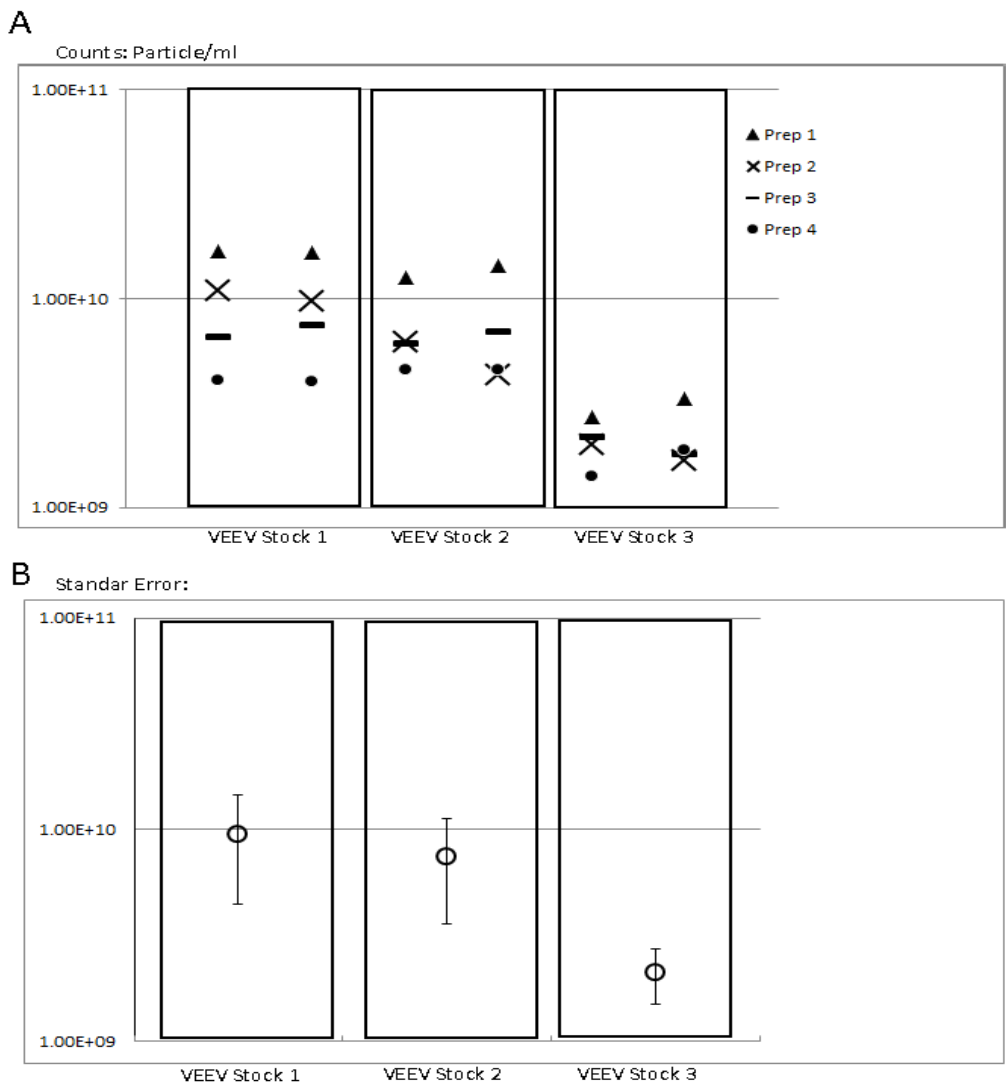


Figure 5

A

Alphavirus Samples	Dilution	STEM-VQ raw concentration (Particle/ml)
EEEV	1:100	5.34E+11
	1:1000	4.38E+10
	1:10000	5.12E+09
WEEV	1:100	5.47E+11
	1:1000	6.19E+10
	1:10000	3.41E+09
VEEV	1:100	3.37E+11
	1:1000	4.43E+10
	1:10000	2.27E+09

B

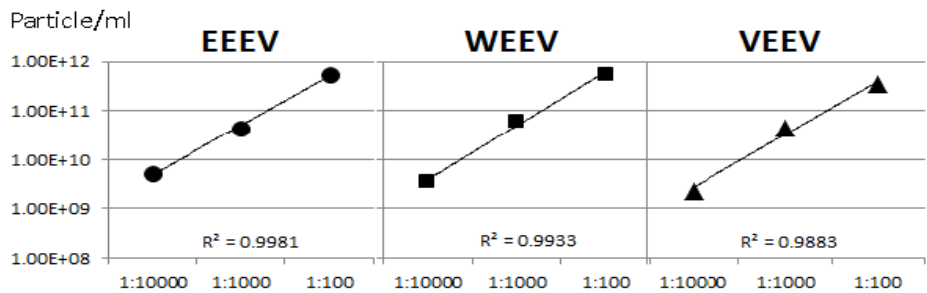
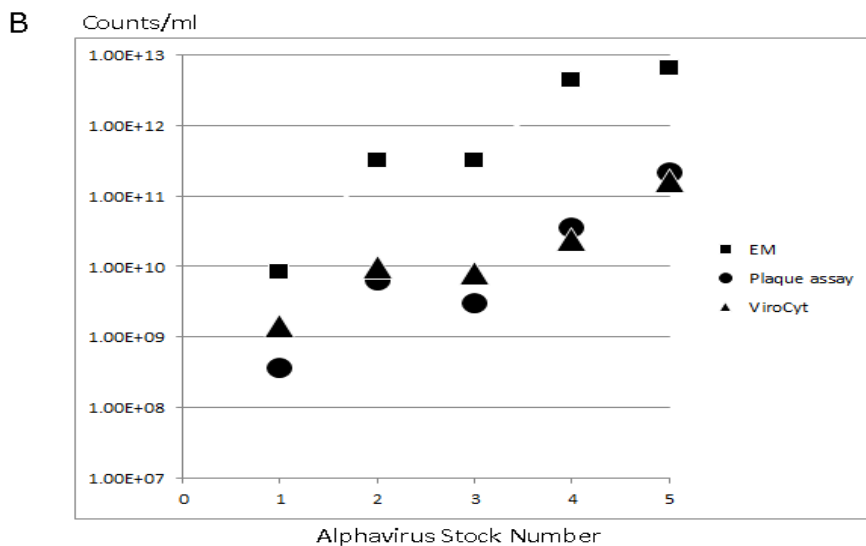
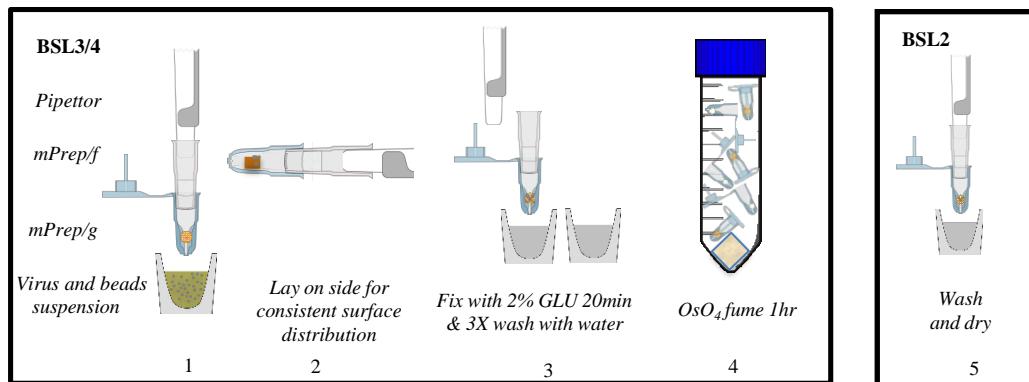


Figure 6

A

Virus Stock	Titer (PFU/ml)	STEM-VQ (P/ml)	ViroCyt (VP/ml)
Stock 1:EEEV MVS	3.68E+08	8.38E+09	1.42E+09
Stock 2:VEEV MVS	6.35E+09	3.23E+11	9.75E+09
Stock 3:VEEV WVS	3.00E+09	3.27E+11	8.09E+09
Stock 4:VEEV SpVS	3.55E+10	4.52E+12	2.45E+10
Stock 5:EEEV SpVS	2.20E+11	6.60E+12	1.62E+11





Supplementary Figure 1: mPrep/g capsule procedure overview: Typical procedure using mPrep system in BSL3/4 biocontainment with short inactivation time. Step 4 can be eliminated if using BSL2 samples.

Conventional TEM method	STEM-VQ method	The Benefits
Grid is exposed to the sample and rinsed by manipulating the grid with forceps.	Once the grid is loaded into the mPrep/g no further grid manipulation is needed for sample exposure and rinsing.	Less damage to the grid which leads to: <ul style="list-style-type: none"> • more even distribution of the virus and beads. • better accuracy. • more data from each grid.
Imaging with TEM.	Imaging with STEM.	STEM imaging is automated which requires much less time. Negative staining is not needed with STEM, due to greater contrast of imaging method with lower voltage.
Manual bead and virus counts.	Image J software for determination of bead and virus counts.	ImageJ analysis requires much less time with greater accuracy.

Supplementary Figure 2: Comparison of conventional TEM method and STEM-VQ method

Supplementary Figure 3: Suggested ImageJ macro codes that were utilized for this study.*For counting 70nm alphavirus:*

```
//set source directory

dir1=getDirectory("Choose Source Directory");

//set directory for masks

dir2=getDirectory("Choose Mask Directory");

//set directory for ImageCalc results

dir3=getDirectory("Choose Results Directory")

//set file list and run for all files in directory

list=getFileList(dir1);

setBatchMode(true);

for (i=0; i<list.length; i++) {

showProgress(i+1, list.length);

filename=dir1+list[i];

if (endsWith(filename, ".tif")) {

open(filename);

//get imageID to pass to Image Calculator

image1=getImageID();

//set image scale

run("Set Scale...", "distance=1 known=4 pixel=1 unit=nm");

run("Subtract Background...", "rolling=150 light");

setAutoThreshold("Default");

//run("Threshold...");

run("Convert to Mask");
```

```
//run watershed to separate particles joined by thresholding

run("Watershed");

run("Analyze Particles...", "size=2000-10000 circularity=0.1-1.00 show=Masks exclude
summarize");

//get imageID of Mask to pass to Image Calculator

image2=getImageID();

saveAs("TIFF", dir2+list[i]);

//need original image prior to running image calculator

open(filename);

image3=getImageID();

//run Image Calculator

imageCalculator("Difference create", image3, image2);

//save Results window

saveAs("TIFF", dir3+list[i]);

close();

run("Close All");

call("java.lang.System.gc");

call("java.lang.System.gc");

call("java.lang.System.gc");

//save summary window to results directory

selectWindow("Summary");

saveAs("Text",dir3+"Summary.txt");

For counting 40nm nano-gold bead particles:

//set source directory
```

```
dir1=getDirectory("Choose Source Directory");

//set directory for masks

dir2=getDirectory("Choose Mask Directory");

//set directory for ImageCalc results

dir3=getDirectory("Choose Results Directory")

//set file list and run for all files in directory

list=getFileList(dir1);

setBatchMode(true);

for (i=0; i<list.length; i++) {

showProgress(i+1, list.length);

filename=dir1+list[i];

if (endsWith(filename, ".tif")) {

open(filename);

//get imageID to pass to Image Calculator

image1=getImageID();

//set image scale

run("Set Scale...", "distance=1 known=4 pixel=1 unit=nm");

run("Subtract Background...", "rolling=150 light");

setAutoThreshold("Default");

//run("Threshold...");

run("Convert to Mask");

//run watershed to separate particles joined by thresholding

run("Watershed");

run("Analyze Particles...", "size=800-1800 circularity=0.5-1.00 show=Masks exclude summarize");
```

```
//get imageID of Mask to pass to Image Calculator
```

```
image2=getImageID();
```

```
saveAs("TIFF", dir2+list[i]);
```

```
//need original image prior to running image calculator
```

```
open(filename);
```

```
image3=getImageID();
```

```
//run Image Calculator
```

```
imageCalculator("Difference create", image3, image2);
```

```
//save Results window
```

```
saveAs("TIFF", dir3+list[i]);
```

```
close();
```

```
run("Close All");
```

```
call("java.lang.System.gc");
```

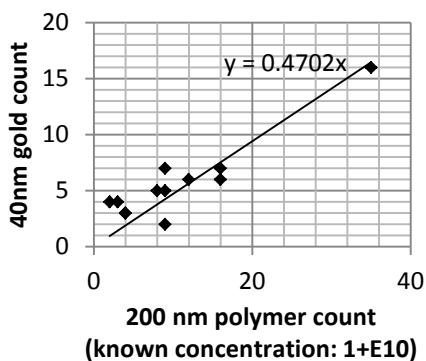
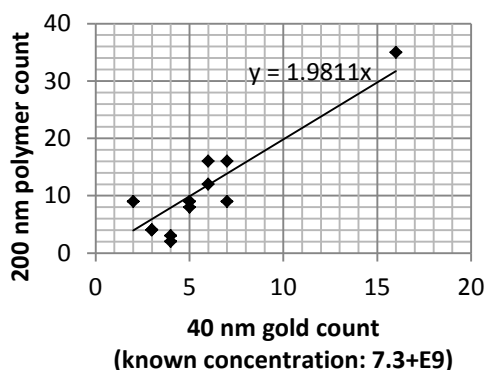
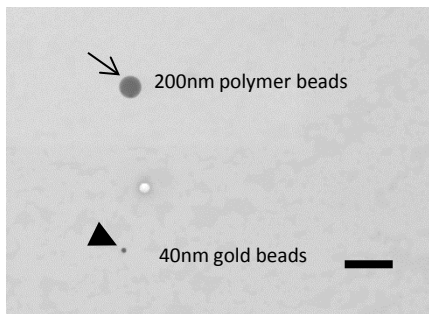
```
call("java.lang.System.gc");
```

```
call("java.lang.System.gc");
```

```
//save summary window to results directory
```

```
selectWindow("Summary");
```

```
saveAs("Text",dir3+"Summary.txt");
```



200nm polymer concentration
 = polymer to gold count ratio × known gold concentration
 = $1.9811 \times 7.3+E9$
 = $1.45+E10$

40nm gold concentration
 = gold to polymer count ratio × known polymer concentration
 = $0.4702 \times 1+E10$
 = $4.7+E9$

Supplementary Figure 4: Using two sets of known concentration beads together to confirm the method accuracy. (A) 200nm polymer beads ($1+E10$ particle/ml, arrow) and 40nm gold beads ($7.3+E9$ particle/ml, arrowhead) were mix equally same volume and apply to EM grid for STEM-VQ count. STEM image, scale bar 400nm. (B) Using 40nm gold concentration to calculate 200nm polymer concentration. Calculated result suggested $1.45+E10$. Compared to the known polymer concentration ($1+E10$), this result was within a log in difference and consider acceptable for accuracy of particle counts. (C) Using 200nm polymer concentration to calculate 40nm gold concentration. Calculated result suggest $4.7+E9$. Compared to the known gold concentration ($7.3+E9$), this result was within a log in difference and consider acceptable for accuracy of particle counts.